Colloid Polym Sci 279:122–130 (2001)

ORIGINAL CONTRIBUTION

Y. Katsumoto
H. Ushiki
A. Graciaa
J. Lachaise

Time evolution of the size distribution of nano-sphere droplets in the hexadecane-in-water miniemulsion stabilized by nonionic surfactants

Received: 1 April 2000
Accepted: 10 August 2000

Y. Katsumoto (✉) · H. Ushiki
Laboratory of Transport and Transformation in Bio-systems
Department of Bio-Mechanics and Intelligent Systems
Graduate School of Bio-Applications and Systems Engineering, Tokyo University of Agriculture and Technology
3–5-8, Saiwai-cho, Fuchu-shi
183–8509 Tokyo, Japan
e-mail: katsumoto@kwansei.ac.jp

A. Graciaa · J. Lachaise
Laboratoire des Fluides Complexes
Université de Pau et des Pays de l'Adour
64000 Pau, France

Abstract Time evolutions of the droplet size distribution in miniemulsions, which is constituted of water/*n*-hexadecane/nonionic surfactants, were investigated by using light scattering techniques. A hard-sphere model is applied to characterize the polydispersity of miniemulsion droplets. Measuring the relative scattering intensity as a function of the volume fraction of dispersed phase, the variance of the droplets size distribution, σ^2, was evaluated. Miniemulsions developed gradually from monodisperse systems ($\sigma^2 \cong 0.02$) to polydisperse ones ($\sigma^2 \geq 0.13$) over 12 days after preparation. σ^2 increased rapidly in the early stage, and ceased to develop at about 6 days after preparation. The *z*-average hydrodynamic radius of miniemulsion droplets grew with time over the whole time range. The change with time of the total droplet number of miniemulsion is in agreement with that predicted by Smoluchowski's theory for diffusion-controlled coagulation. Although the characteristic coagulation time obtained here was much larger than that estimated by Smoluchowski's theory, the qualitative agreement between the theory and the experimental results obtained here is good. At the earlier stage of the destabilization process of miniemulsions, the growth mechanism of droplets may be explained in terms of a diffusion-controlled coagulation.

Key words Miniemulsion · Light scattering · Diffusion-controlled coagulation · Droplet size distribution function · Time evolution of polydispersity

Introduction

In general, making small droplets of a submicrometer in radius takes a large amount of energy. In many cases a high pressure homogenizer is required. Recently, we have developed a thermal protocol that allows us to produce bluish oil in water (O/W) emulsions under gentle stirring or agitation [1]. The characteristic size of the O/W emulsion droplets obtained is of the order of 10 nm. Although these features are quite similar to those for a microemulsion, the system obtained is not thermodynamically stable. That is, the bluish O/W emulsion becomes milky, and reaches a thermodynamically equilibrium state with time. In order to distinguish the O/W emulsion obtained from microemulsions that are thermodynamically stable, this emulsion has been called a "miniemulsion". In previous papers [2–4], the physical properties and time evolution of the miniemulsion constituted of water/*n*-hexadecane/heptaethylene glycol mono-*n*-dodecyl ether ($C_{12}EO_7$) was investigated by using light scattering techniques and fluorescent probe methods. The miniemulsion obtained changes phase to Winsor's I phase gradually, i.e., the miniemulsion separates into two phases after a certain time interval. At the initial state, miniemulsion droplets undergo hard sphere interaction in terms of the

Percus-Yevick approximation [2]. The droplet radius of the miniemulsion obtained was about 10 nm, and the ratio of the hydrodynamic radius to the hard sphere radius was about 1.2. Note that the miniemulsions prepared are bluish because of the existence of the strong repulsive interaction between droplets. Also, it was suggested that the water bound on miniemulsion droplets plays an important role in producing a homogeneous miniemulsion. Using fluorescence probe techniques, the miscibility of the internal phase of miniemulsion droplets was investigated [4]. Results indicated that the internal phase of miniemulsion droplets is miscible without changing the droplet radius. This mixing process is very fast compared with the destabilizing process of miniemulsion droplets observed by the use of light scattering techniques.

When water to oil ratio (WOR) is varied from 4–10, a bluish O/W emulsion (so-called "miniemulsion") was produced, while an opaque O/W emulsion was obtained when WOR is equal to 3. The physical properties of miniemulsions are different from the opaque O/W emulsions with WOR = 3 as reported our previous papers [2, 3]. In these systems, the increase of the droplet radius was investigated over 24 days after preparation. When the opaque O/W emulsion was obtained, the cube of the z-average hydrodynamic radius r_z^3 was varied linearly with time over the whole time range. On the other hand, two distinct regimes in the growth process were found in miniemulsion systems ($4 < \mathrm{WOR} < 10$). In these papers, the growth process of miniemulsions was discussed in terms of Ostwald ripening, and the following features were suggested:

1. In the earlier stages, r_z^3 varied linearly with time. Initially the droplet size distribution function was narrow, and then it broadened at 12 days after preparation (the variance of the observed distribution was larger than 0.15). The growth rate of the earlier stages was smaller than that observed latter.
2. In the latter stage, r_z^3 varies linearly with time. At 22 days after preparation the droplet size distribution became narrow again. The observed growth rate in the latter stages was in agreement with the theory for Ostwald ripening.

The latter stages may be explained in terms of Ostwald ripening as indicated in our previous paper [3]. With regard to the earlier stages, however, more detailed investigation is required in order to reveal the growth mechanism of miniemulsion droplets.

In this present work, the time evolution of the droplet size distribution was investigated over 12 days after preparation. The hard sphere fluid theory [5–8] was applied to predict the polydispersity of miniemulsion droplets, derived from light scattering experiments [9–14]. Our experimental data therefore helps us to understand the growth mechanism of miniemulsion droplets in the earlier stage.

Experimental

Materials

Mergital LT7 (main component is heptaethylene glycol mono-*n*-dodecyl ether, $C_{12}E_7$) was furnished by Sidobre Sinnova, *n*-hexadecane was purchased from Fluka. All materials were used without further purification. The distilled water was used in the preparation of emulsions.

Methods

Sample preparation. Referring to PIT (Phase Inversion Temperature) method proposed by Shinoda and Saito [15], a stock miniemulsion is prepared by a thermal protocol under gentle stirring. The role of PIT for the preparation of stock miniemulsions was described previously (see Sect. 3.1. in our previous paper [2]). The volume ratio of water to oil (WOR) was fixed at 4 and 9, and the surfactant mass fraction was 0.12 in all samples. The stock miniemulsions had been maintained under a temperature of 25 °C after preparation. The volume fraction of the dispersed phase ϕ' is calculated by the fraction of oil and surfactant volume (V_o and V_s) to the total volume as

$$\phi' = \frac{V_o + V_s}{V_o + V_s + V_w} \tag{1}$$

where V_w denotes the total water volume. V_s was calculated by dividing the surfactant mass by its density $\rho_s = 0.998$. At the preparation of stock miniemulsions, the volume fraction of each component (V_o, V_s, and V_w) must be fixed. So ϕ' of a stock miniemulsion, ϕ'_0, is characteristic. For miniemulsions of WOR = 4 and 9, ϕ'_0 are equal to 0.2924 and 0.2061, respectively.

Light scattering measurements. Light scattering measurements were accomplished by using a device which is constructed by a He-Ne laser ($\lambda = 632.8$ nm) of 15 mW, a photon counting photomultiplier and a MALVERN 7032 Multi-8 with 64 channels as the digital correlator. The homodyne method was employed. All experiments were performed at a scattering angle of 90°, and at a temperature of 25 °C. For relative scattering intensity measurements, the stock miniemulsions maintained at 25 °C was stepwise diluted with the disperse medium (the distilled water). Varying ϕ' from ϕ'_0 to 0.01, the relative scattering intensity was measured. In some cases the angle was varied between 60° and 120°, but there is no angular dependence of the scattering intensity.

The dynamic light scattering measurements were carried out under a condition of infinite dilution. The stock miniemulsions were diluted by the dispersion medium about 30 min before each measurement. The volume fraction of the stock miniemulsion in water was about 0.01. In the previous paper [2] no angular dependence of the z-averaged hydrodynamic radius of miniemulsion droplets was confirmed in such a dilute solution. The relationship between the normalized first-order electric field autocorrelation function $g^{(1)}(q,\tau)$ and the single-clipped photoelectron-count autocorrelation function $g^{(2)}(q,\tau)$ is represented by [16]

$$g^{(2)}(q,\tau) = B\left(1 + \beta\left|g^{(1)}(q,\tau)\right|^2\right) \tag{2}$$

where q is the scattering vector $q = (4\pi n_0/\lambda)\sin(\theta/2)$, β is the coherent factor which dependent on instrumental conditions, and B is the base line. n_0, λ, and θ denote the refractive index of the disperse medium (water), the wavelength of the incident light, and the scattering angle, respectively. From the dynamic light scattering

experiments, a z-averaged diffusion coefficient D_z was estimated by means of a second-order cumulant analysis [17]. The z-averaged radius of dispersed droplets, r_z, is calculated by Stokes-Einstein relation: $r_z = kT/6\pi\eta D_z$, where k, T, and η denote Boltzmann's constant, the absolute temperature, and the viscosity of the disperse medium, respectively. Using a non-linear least square method [18], we made curve fitting programs using PASCAL (Borland: Turbo PASCAL) based on the quasi-Marquardt algorithm. These calculations were carried out on a personal computer (PC-9821Xn).

Result and discussion

Relative scattering intensity measurements

The variations of the relative scattering intensity I^{rel} with ϕ' are shown in Fig. 1 (for the miniemulsion of WOR = 4) and 2 (WOR = 9). The data were measured over 12 days after preparation of stock miniemulsions. In the miniemulsion of WOR = 4, however, it was hard to obtain the variation of I^{rel} with ϕ' after 8 days, because at higher ϕ' the contributions from multiple scattering could not be neglected. It is worth noting that the creaming of these samples, i.e., the phase separation, is observed at 1 or 2 months after the preparation. I^{rel} rises linearly, then flattens off, passes a maximum, to decrease monotonically with further increasing ϕ'. Similar curves were found by several researchers, for example in the quaternary ionic microemulsions [11, 12], in the decane-in-water microemulsion stabilized by pentaethylene glycol mono-*n*-dodecyl ether ($C_{12}E_5$) [13], and in the octane-in-water microemulsion stabilized by $C_{12}E_5$ [14]. The variation of I^{rel} with ϕ' has a peak near $\phi' = 0.08$ for miniemulsion of WOR = 9, and near $\phi' = 0.12$ for miniemulsion of WOR = 4 at 0 days. The relative scattering intensity increased, and the peak position shifts to a high ϕ' with time. In the previous paper [2] we discuss the application of the hard sphere fluid theory to the analysis of this kind of scattering profile obtained from the same system in detail.

In order to analyze the scattering profiles obtained here, a theoretical representation for the variation of I^{rel} with the volume fraction of dispersed droplets ϕ proposed by Vrij and co-workers [9, 10] was employed. The relative scattering intensity as a function of ϕ is expressed as follows [2]:

$$I^{\mathrm{rel}}(\phi) \sim \frac{4\pi^2 n_s^2}{\lambda^4}\left(\frac{\partial n_s}{\partial \phi}\right)^2 \phi \left(\frac{\partial}{\partial \phi}\frac{\Pi}{kT}\right)^{-1} \tag{3}$$

where n_s is the refractive index of the solution, and Π is the osmotic compressibility. When miniemulsion droplets have the interaction potential due to hard sphere repulsion, Π/kT can be written by Hiroike-Baxter solution for the Percus-Yevick approximation [7, 8]:

$$\frac{\Pi}{kT} = \frac{6}{\pi}\left\{\frac{\xi_0}{1-\xi_3} + \frac{3\xi_1\xi_2}{(1-\xi_3)^2} + \frac{3\xi_2^3}{(1-\xi_3)^3}\right\} \tag{4}$$

In a polydisperse system, ξ_v is represented by

$$\xi_v = \frac{4\pi}{3}\sum_{i=1}^{n}\rho_i r_i^v = \frac{\mathrm{M}_v}{\mathrm{M}_3}\phi\bar{r}^{v-3} \tag{5}$$

where ρ_i is the number density of the i-th species droplet, r_i is the radius of the i-th species droplet, and $\bar{r}$ is the average radius of the droplets. M_v is the normalized radius moment defined as $\mathrm{M}_v = \overline{r^v}/\bar{r}^v$. $\overline{r^v}$ is the radius moments defined as

$$\overline{r^v} = \sum_i N_i r_i^v / \sum_i N_i \tag{6}$$

where N_i is the number of the i-th species droplet. ϕ is the volume fraction of dispersed droplets calculated by

$$\phi = \frac{4\pi}{3}\sum_{i=1}^{n}\rho_i r_i^3 \tag{7}$$

In this case Vrij et al. [9, 10] proposed the following equation for the osmotic compressibility of a concentrated and polydisperse colloidal suspension:

$$\left(\frac{\partial}{\partial\phi}\frac{\Pi}{kT}\right)^{-1} = \frac{4\pi}{3}\bar{r}^3\frac{(1-\phi)^4}{(1+2\phi)^2}\left[1 - \frac{9\phi}{(1-\phi)^2}\left\{1 - \frac{\mathrm{M}_4^3}{\mathrm{M}_3^2\mathrm{M}_6}\right\} + \frac{6\phi(1+2\phi)}{(1-\phi)^2}\left\{1 - \frac{\mathrm{M}_4\mathrm{M}_5}{\mathrm{M}_3\mathrm{M}_6}\right\}\right] \tag{8}$$

If we expect a logarithmic-normal type as the droplet size distribution function, the following expression is used as M_v [10]:

$$\mathrm{M}_v = \left(1+\sigma^2\right)^{v(v-1)/2} \tag{9}$$

where σ^2 denotes the variance of the distribution of hard sphere radii. There is no certain reason to adapt the hypothesis that the size distribution of miniemulsion droplets is a logarithmic normal type. However, Eq. (9) was employed from the following reasons: (i) many researchers have found the size distribution function of logarithmic normal type in emulsion systems [1]; (ii) it is beneficial to postulate a type of the distribution function in order to reduce the number of fitting parameters. Moreover it is difficult to discuss the higher order terms of the radius moment independently based on a fitting result for these experimental data obtained here. Substitution of Eq. (9) into Eq. (8) gives

$$\left(\frac{\partial}{\partial\phi}\frac{\Pi}{kT}\right)^{-1} = \frac{4\pi}{3}\bar{r}^3\frac{(1-\phi)^4}{(1+2\phi)^2}\left[1 - \frac{9\phi}{(1-\phi)^2}\left\{1 - \frac{1}{(1+\sigma^2)^3}\right\} + \frac{6\phi(1+2\phi)}{(1-\phi)^2}\left\{1 - \frac{1}{(1+\sigma^2)^2}\right\}\right] \tag{10}$$

Equations (3) and (10) yield the following equation:

$$I^{rel}(\phi) = \varphi'\phi\frac{(1-\phi)^4}{(1+2\phi)^2}\left[1-\frac{9\phi}{(1-\phi)^2}\left\{1-\frac{1}{(1+\sigma^2)^3}\right\}+\frac{6\phi(1+2\phi)}{(1-\phi)^2}\left\{1-\frac{1}{(1+\sigma^2)^2}\right\}\right] \quad (11)$$

which clearly reduces to the expected result for a monodisperse system (Eq. (20) in [2]) when $\sigma^2 = 0$. φ' is an adjustable parameter in the fitting procedure. When $\sigma^2 = 0$, $I^{rel}(\phi)$ increases linearly at lower ϕ, passes a maximum at $\phi = 0.129$, to then decrease monotonically to zero at $\phi = 1$. The peaks of the observed I^{rel} at 0 days were shifted to a low ϕ' as shown in Figs. 1 and 2. In the fitting procedure, therefore, it was assumed that the volume fraction of dispersed droplets is proportional to that of dispersed phase: $\phi = \alpha\phi'$. This item was discussed in our previous paper [2]. The full lines in Figs. 1 and 2 represent the fitting result using Eq. (11). The evaluated values for σ^2 and α are listed in Tables 1 and 2.

For the miniemulsion of WOR = 4, α increased over 5 days, then it reached a constant value (Table 1). For the miniemulsion of WOR = 9, on the other hand, α shows no significant dependence on time over 12 days. According to our previous paper [2], α is concerned with the amount of bound water on miniemulsion droplets. It is therefore presumed that the amount of bound water on miniemulsion droplets changed with time in the miniemulsion with WOR = 4. In order to

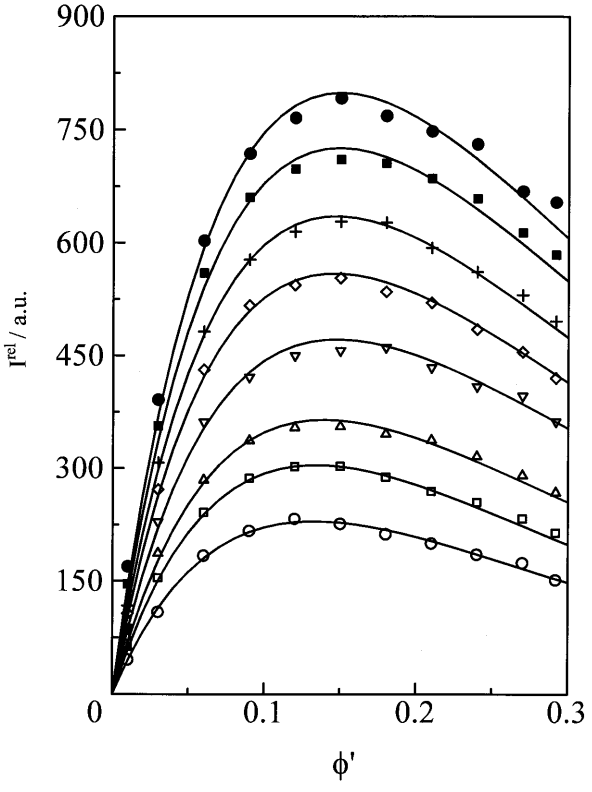

Fig. 1 Temporal change of I^{rel} with ϕ' for miniemulsion of WOR = 4 at 0 days (*open circles*), 1 day (*open squares*), 2 days (*open triangles*), 3 days (*open reversed triangles*), 4 days (*open diamonds*), 5 days (*crosses*), 6 days (*filled squares*) and 7 days (*filled circles*) after preparation. The *full lines* are the results of the theoretical fit with using Eq. (9)

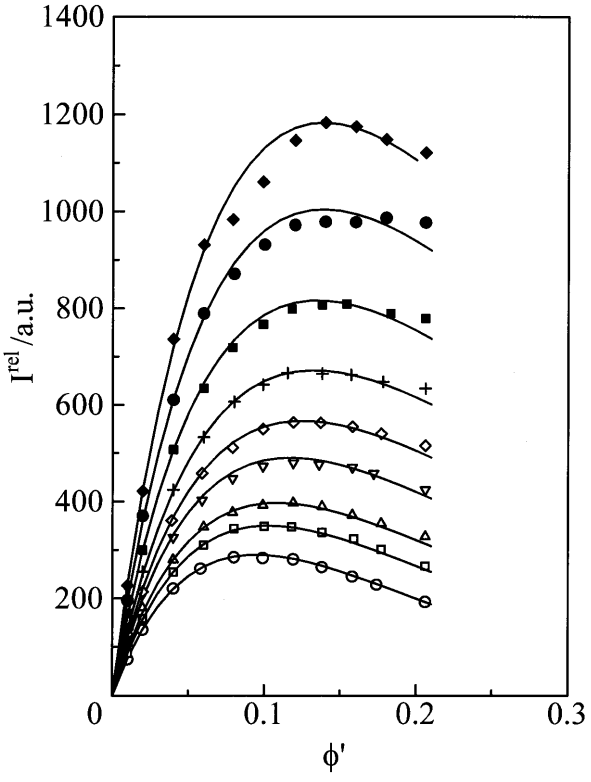

Fig. 2 Temporal change of I^{rel} with ϕ' for miniemulsion of WOR = 9 at 0 days (*open circles*), 1 day (*open squares*), 2 days (*open triangles*), 3 days (*open reversed triangles*), 4 days (*open diamonds*), 6 days (*crosses*), 8 days (*filled squares*), 10 days (*filled circles*) and 12 days (*filled diamonds*) after preparation. The *full lines* are the results of the theoretical fit with using Eq. (9)

Table 1 σ^2, α and r_z derived from relative scattering intensity measurements and dynamic light scattering measurements in the miniemulsion of WOR = 4

Days	σ^2	α	r_z ($\times 10^{-9}$ m)
0	0.029	1.04	11.9
1	0.039	1.06	12.9
2	0.070	1.12	15.1
3	0.102	1.14	15.5
4	0.110	1.16	17.7
5	0.121	1.17	–
6	0.132	1.17	19.4
7	0.135	1.17	–
8	–	–	20.8
10	–	–	22.0
12	–	–	25.5

confirm this assumption, however, a temporal change of the association between water molecules and poly(ethylene oxide) chains of $C_{12}EO_7$ in miniemulsions must be investigated by using the other experimental technique. We postpone the question until more detailed data are obtained.

Temporal change of the droplet size distribution of miniemulsions

Figure 3 represents the variation of the obtained σ^2 with time. Time dependence of σ^2 indicates that miniemulsions developed from the monodisperse system to polydisperse one. At the initial time ($t = 0$ day), we obtain $\sigma^2 = 0.029$ and 0.011 for the miniemulsions of WOR = 4 and 9, respectively. These values for σ^2 are quite similar to the reported one in the system of O/W microemulsions stabilized by non-ionic surfactants [14, 19]. That is to say, the stock miniemulsions are apparently homogeneous systems like a microemulsion at the initial state. Then σ^2 increased rapidly and seems to approach a constant value after a certain time interval.

On the other hand, the z-average hydrodynamic radius of miniemulsion droplets, r_z, increased gradually in the whole time range. Figures 4 and 5 show the obtained $g^{(1)}(\tau)$ at 0 days and 12 days after preparation of miniemulsion WOR = 4 and WOR = 9, respectively. The solid lines represent the fitting results by using second-order cumulant analysis. Note that the estimated second-order moments varied between 0.01 and 0.1, but an obvious tendency could not be found. Therefore the temporal changes in r_z are discussed using the experimental result from dynamic right scattering measurements. Figure 6 suggests that the miniemulsion droplets grew larger over 12 days. The variance of the droplet size distribution function stopped increasing at a certain point before 12 days.

Using the values for σ^2 and α listed in Tables 1 and 2, the droplet size distribution, s(r), can be estimated. The following logarithmic-normal type is assumed as the droplet size distribution [20]:

Table 2 σ^2, α and r_z derived from relative scattering intensity measurements and dynamic light scattering measurements in the miniemulsion of WOR = 9

Days	σ^2	α	r_z ($\times 10^{-9}$ m)
0	0.0111	1.4	7.35
1	0.0486	1.41	8.20
2	0.0772	1.42	9.40
3	0.115	1.42	10.8
4	0.1504	1.42	12.5
5	0.1804	1.41	–
6	0.1914	1.41	13.9
8	–	–	15.8
10	0.201	1.39	16.4
12	0.2062	1.4	17.9

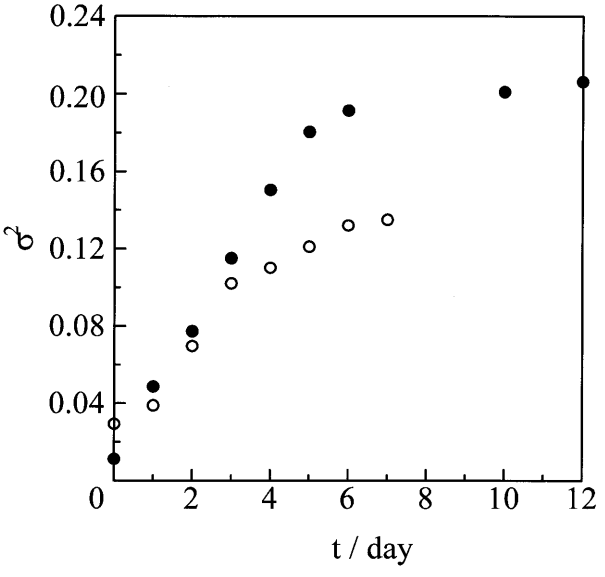

Fig. 3 Temporal change in σ^2 for miniemulsions of WOR = 4 (*open circles*) and WOR = 9 (*filled circles*)

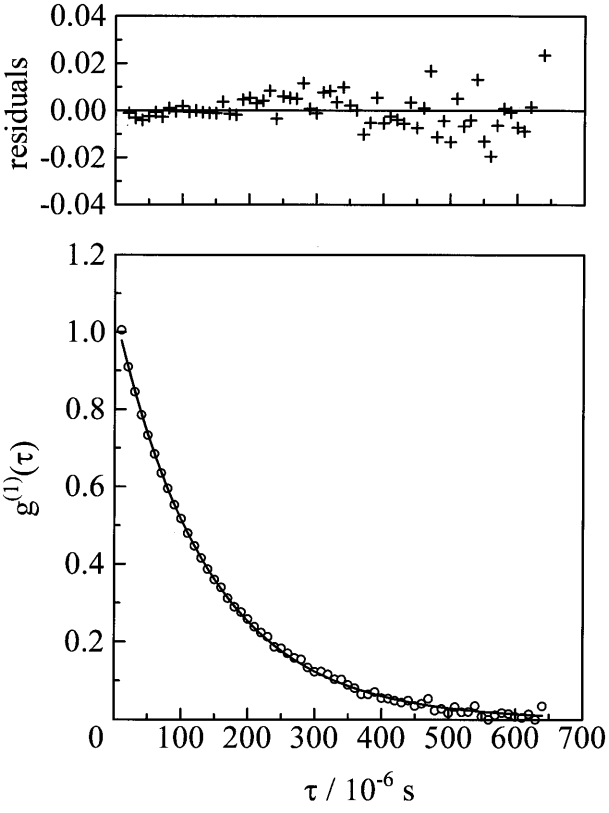

Fig. 4 $g^{(1)}(\tau)$ of the miniemulsion with WOR = 4 at 0 days. The *solid line* represents the fitting result by the second-order cumulant analysis

$$s(r) = \frac{1}{\sqrt{8\pi}\sigma r}\exp\left[-\frac{1}{2}\left(\frac{\ln r - \ln \bar{r}}{\sigma}\right)^2\right] \quad (12)$$

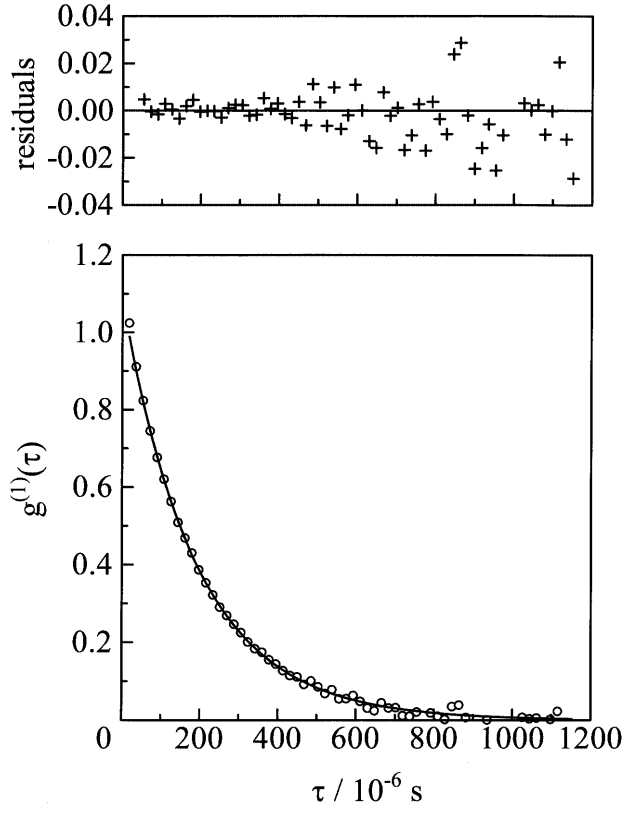

Fig. 5 $g^{(1)}(\tau)$ of the miniemulsion with WOR = 9 at 12 days. The *solid line* represents the fitting result by the second-order cumulant analysis

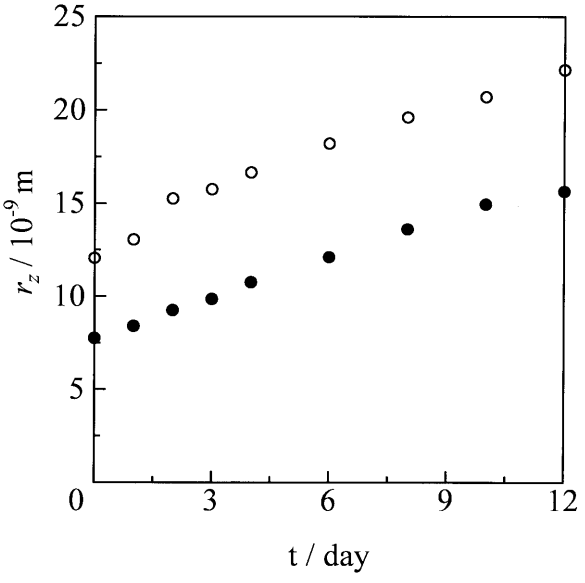

Fig. 6 Variation of r_z with time for miniemulsions of WOR = 4 (*open circles*) and WOR = 9 (*filled circles*)

where r is the droplet radius. $\bar{r} = r_z$ was assumed in the calculation. The temporal change in the droplet size distribution of miniemulsions, s(r), is shown in Fig. 7.

Growth mechanism of miniemulsion droplets

The time evolution of the droplet size distribution of miniemulsion was investigated in the above sections. The following features of the growth process of miniemulsion droplets were pointed out:

1. The droplet size of miniemulsions increases gradually with time over 12 days.
2. The variation of the droplet size distribution is very low initially and rises rapidly until about 6 days after preparation. Then it ceases to increase and approaches a certain value.

First, in order to discuss the growth mechanism of miniemulsion droplets, the temporal change in the total

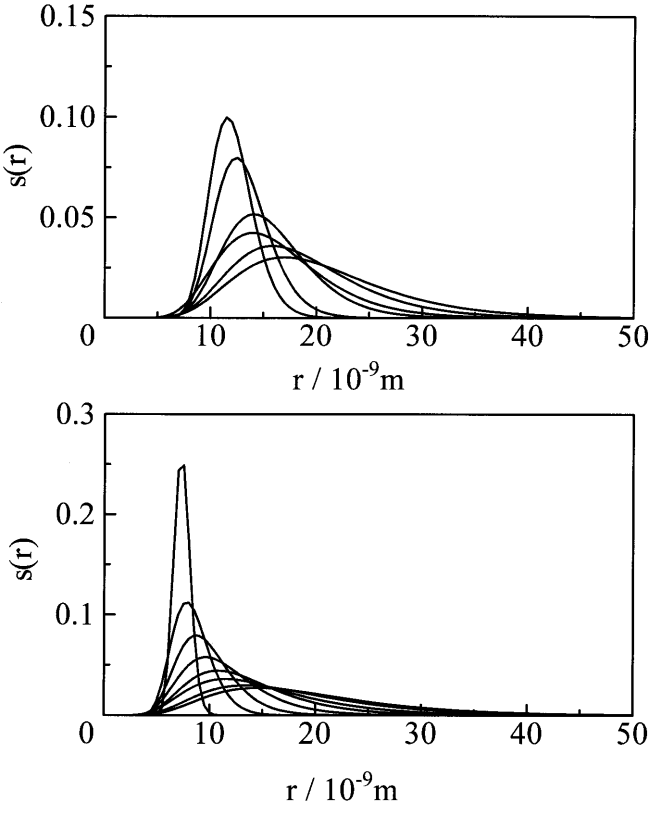

Fig. 7 Temporal change in the droplet size distribution for miniemulsions of WOR = 4 (*top*) and WOR = 9 (*bottom*) calculated by Eq. (10) using σ^2 and r_z listed in Tables 1 and 2. The *solid lines* from the narrow one to the broad one in the top figure are the estimated distributions for 0 days (the narrowest one), 1 day, 2 days, 3 days, 4 days, and 6 days (the broadest one) after preparation, respectively. At the *bottom*, the *solid lines* represent the estimated distributions for 0 days (the narrowest one), 1 day, 2 days, 3 days, 4 days, 6 days, 10 days, and 12 days (the broadest one) after preparation, respectively

number of miniemulsion droplets N(t) was estimated using the calculated distribution function (shown in Fig. 7):

$$\mathrm{N}(t) = \frac{3\phi}{4\pi} \sum_{i=1}^{\mathrm{n}} \frac{\mathrm{s}(r_i, t)}{r_i^3} \tag{13}$$

ϕ was determined by use of the values listed in Tables 1 and 2. Figure 8 shows the time dependence of N(t)/N(0). The N(t)/N(0) obtained decreases monotonically with time. When the growth mechanism of droplet is caused by a diffusion controlled process, N(t)/N(0) should be represented by the following equation [23]:

$$\frac{\mathrm{N}(t)}{\mathrm{N}(0)} = \frac{1}{1 + t/\tau} \quad , \tag{14}$$

where τ is a characteristic growth rate. The full line in Fig. 8 was drawn using Eq. (14) with $\tau = 2.4$ days. Good agreement between experimental data and the theoretical curves was found.

In our previous paper [3], two distinct regimes were observed in temporal change in the destabilization process of miniemulsion droplets, and the following schemes of the growth mechanisms for the earlier and latter stages were inferred:

1. At the earlier stage, r_z^3 varies linearly with time. At an initial time, the droplet size distribution function is narrow, then it broadens at 12 days after preparation. The growth mechanism of the first stage may deviate from the fundamental mechanism of Lifshitz-Slezov-Wagner (LSW) theory [21, 22] for Ostwald ripening.

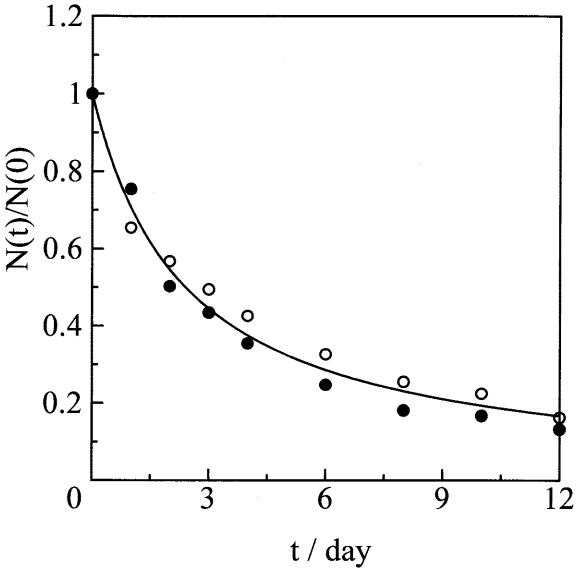

Fig. 8 Variation of N(t)/N(0) with time for miniemulsion of WOR = 4 (*open circles*) and WOR = 9 (*filled circles*). The *full line* was calculated by means of Eq. (12) using $\tau = 2.4$ days

2. At the latter stage, r_z^3 varies linearly with time. At 22 days after preparation, the droplet size distribution again approaches the time-independent form predicted by LSW theory. Fundamental mechanisms of LSW theory were found out at the latter stage.

In the present paper, stage 1 is investigated measuring the temporal change in σ^2 of the stock miniemulsion. The results may suggest that the growth process of stage 1 can be explained in terms of the diffusion-controlled coagulation [23]. The variation in the population of droplets that has a certain radius, n(r), with time was estimated by using the calculated distribution functions represented in Fig. 5. The left of Fig. 7 represents the temporal change in n(r) for the miniemulsion of WOR = 9, and the right shows the theoretical curves calculated by the following equation [23]:

$$n_k = N_t(0) \frac{(t/\tau)^{k-1}}{(1 + t/\tau)^{k+1}} \tag{15}$$

where n_k denotes the number of the aggregates comprising k droplets ($k = 1, 2, \ldots$). Note that n_1 represents the number of the single particles. Figure 9 shows the comparison between n(r) and n_k. In order to compare n(r) with n_k, $N_t(0) = 0.25$ and $\tau = 2.4$ days were used. The graphs on the left represent the temporal change in the normalized number of the droplet, n(r), where $r = 7.5$ nm (top), 16 nm, 20 nm, and 25 nm (bottom), calculated from the droplet size distributions represented in Fig. 7. The graphs on the right are the temporal change in the normalized number of the aggregates comprising k ($k = 1$ (top), 2, 3, 4, and 5(bottom)) droplets calculated by using Eq. (15). The comparison shown in Fig. 9 is not a strict one, because the aggregation number of droplets in an aggregate was unknown in the light scattering experiment. However, one can consider that the temporal change of n(r) is similar to that of n_k, especially in the figures for $r = 7.5$ nm and 9.5 nm. The qualitative agreement between the theory and the experimental results is then good. This implies that the miniemulsion is destabilized by the diffusion-controlled coagulation process at stage 1.

In this case, the variation of σ with time may be explained by the self-preserving behavior on particle size distributions in the diffusion-controlled coagulation kinetics reported by Friedlander et al. [24, 25] and Hidy [26]. The coagulation process of hydrosols [22] and aerosols [23] was investigated theoretically and experimentally. They suggested that the normalized size distributions of coagulating particles tend to preserve their shape after a sufficiently long time. That is to say, the variance of the normalized size distribution ceases to develop after a certain time interval, when the type of the size distribution function does not change with time. Also they indicated that this tendency is independent of the initial distribution. Although the τ obtained here was

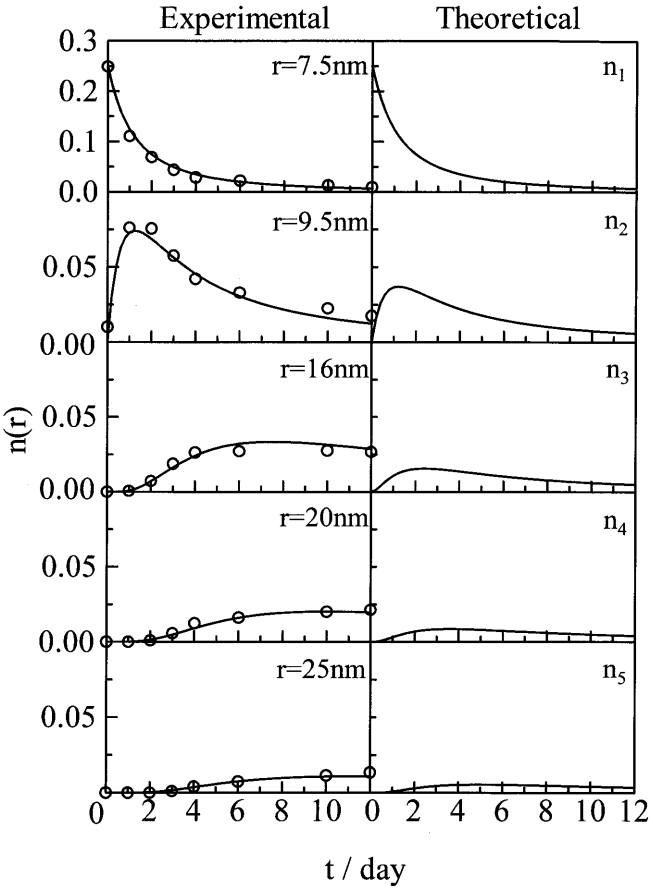

Fig. 9 The comparison between n(r) and n_k. Left: temporal change in the normalized number of the droplet, n(r), in which $r = 7.5$ nm (*top*), 16 nm, 20 nm, and 25 nm (*bottom*), calculated from the droplet size distributions represented in Fig. 7. Right: temporal change in the normalized number of the aggregates comprising k ($k = 1$ (*top*), 2, 3, 4, and 5 (*bottom*)) droplets calculated by using Eq. (15)

much smaller than that predicted by Smoluchowski's theory as discussed in our previous paper [3], the temporal change in n(r) shows quite similar behavior to n_k predicted by Smoluchowski's theory [23]. If the growth mechanism of miniemulsion droplets at earlier stage is explained in terms of the diffusion-controlled coagulation, the observed small values for τ may be ascribed to the effect of a strong repulsion between droplets caused by the steric stabilization of nonionic surfactants [2].

Considering the previous paper [3] and the present work, the following scheme on the destabilization process of miniemulsion can be proposed. Just after the preparation of miniemulsion, droplets have a strong repulsive interaction in terms of Percus-Yevick approximation. The droplets radius increases with time and the droplet distribution broadens over about 8 days by the diffusion-controlled coagulation process. After about 10 days, the system obeys Ostwald ripening process with LSW theory.

Although we could obtain the overview of the growth mechanism of miniemulsion, more detailed data should be obtained in order to reveal the evolutionary behavior of miniemulsions. It is desirable to investigate the observed anomalous values for τ, the exchange process of the internal phase of miniemulsion droplets, and so on.

Conclusion

The light scattering techniques permits characterizing the polydispersity of a miniemulsion, which is constituted of nano-sphere droplets. Measuring the relative scattering intensity as a function of the volume fraction of dispersed phase, the variance of the droplets size distribution, σ^2, was evaluated by means of the hard sphere fluid model. The temporal change in the variance of the droplet size distribution and the z-averaged hydrodynamic radius of miniemulsion was investigated over 12 days after preparation. Miniemulsions developed gradually from a monodisperse system ($\sigma^2 \cong 0.02$) to a polydisperse one ($\sigma^2 \geq 0.13$). σ^2 increased rapidly at the early stage, and ceased to develop at about 6 days after preparation. The z-average hydrodynamic radius of miniemulsion droplets grew with time over the whole time range. The temporal change of the total droplet number of miniemulsion is in agreement with Smoluchowski's theory for the diffusion-controlled coagulation. But the characteristic coagulation time obtained here was much larger than that estimated by the theory. The broadening of the droplet size distribution is a characteristic feature of the diffusion-controlled coagulation process. At the earlier stages of the destabilization process of miniemulsions, the growth mechanism of miniemulsion droplets may be explained by means of the diffusion-controlled coagulation process.

References

1. Sing AJF, Graciaa A, Lachaise J, Brochette P, Salager JL (1999) Colloids Surf A 152:31–39
2. Katsumoto Y, Ushiki H, Graciaa A, Lachaise J (2000) J Phys Condens Matter 12:249–264
3. Katsumoto Y, Ushiki H, Mendiboure B, Graciaa A, Lachaise J (2000) J Phys Condens Matter 12:3569–3583
4. Katsumoto Y, Ushiki H, Mendiboure B, Graciaa A, Lachaise J (2000) Colloid Polym Sci 278:905–909
5. Wertheim MS (1963) Phys Rev Lett 10: 321–323
6. Thiele E (1963) J Chem Phys 39:474–479
7. Hiroike K (1969) J Phys Soc Japan 27:1415–1421

8. Baxter RJ (1970) J Chem Phys 52: 4559–4562
9. Vrij A (1978) J Chem Phys 69:1742–1747; Vrij A (1978) Chem Phys Lett 53: 144–147; Vrij A (1982) J Colloid Interface Sci 90:110–116
10. Pusey PN, Fijnaut HM, Vrij A (1982) J Chem Phys 77:4270–4281
11. Agterof WGM, van Zomeren JAJ, Vrij A (1976) Chem Phys Lett 43:363–367
12. Cazabat AM, Langevin D, Pouchlon A (1980) J Colloid Interface Sci 73:1–12
13. Olsson U, Schurtenberger P (1993) Langmuir 9:3389–3394
14. Kahlweit M, Strey R, Sottmann T, Busse G, Faulhaber B, Jen J (1997) Langmuir 13:2670–2674
15. Shinoda K, Saito H (1968) J Colloid Interface Sci 26: 70; Shinoda K, Saito H (1969) J Colloid Interface Sci 30:258
16. See, for instance, Berne BJ, Pecora R (1976) Dynamic light scattering. Wiley, New York
17. Koppel DE (1972) J Chem Phys 57: 4814–4820
18. Nakagawa T, Oyanagi Y (1982) Saishou Nijou-hou niyoru Jikken-Data Kaiseki. Tokyo Daigaku Syuppan-kai, Tokyo
19. Fletcher PDI, Johannsson R (1994) J Chem Soc Faraday Trans 90: 3567–3572
20. Yan YD, Clarke JHR (1989) Adv Colloid Interface Sci 29:277–318
21. Lifshitz IM, Slezov VV (1959) Sov Phys JETP 35: 33; Lifshitz IM, Slezov VV (1961) J Phys Chem Solid 19:35
22. Wagner C (1961) Z Electrochem 35: 581
23. von Smoluchowski M (1916) Physik Zeitschr 17: 557, 583; von Smoluchowski M (1917) Z Physik Chem 92:129
24. Swift DL, Friedlander SK (1964) J Colloid Sci 19:621
25. Friedlander SK, Wang CS (1966) J Colloid Interface Sci 22:126; Lai FS, Friedlander SK, Pich J, Hidy GM (1972) J Colloid Interface Sci 39:395
26. Hidy GM (1965) J Colloid Sci 20:123